The Di-iron Oxygenase PhnZ

## Jacqueline P Séguin and David L Zechel

Department of Chemistry, Queen's University, Kingston, Ontario, K7L 3N6, Canada

FUNCTIONAL CLASS

Enzyme; 1-hydroxyalkylphosphonic acid, Fe(II)-dependent monooxygenase; EC 1.13.99.

PhnZ is a bacterial enzyme that utilizes molecular oxygen and a pair of iron atoms to catalyze the oxidative cleavage of the carbon–phosphorus (CP) bond in (R)-2-amino-1-hydroxyethylphosphonic acid (**1**) to yield glycine and inorganic phosphate (Pi) (Scheme 1(a)).[2] PhnZ is formally a monooxygenase rather than a dioxygenase as only one atom of molecular oxygen is incorporated into the substrate during catalysis, as demonstrated by mass spectrometric (MS) analysis of reactions run with $^{18}O_2$.[3] This is a four-electron oxidation as the alcohol in **1** is converted to an acid. The iron atoms are in a mixed-valence Fe(II)/Fe(III) oxidation state for catalysis and do not require a supply of external electrons for turnover as the cofactor returns to the Fe(II)/Fe(III) state at the end of each cycle.[3] This is because the two electrons donated by the cofactor to activate molecular oxygen are reacquired from the substrate during CP-bond cleavage. This is in contrast to other di-iron-dependent monoxygenases, such as methane monooxygenase, which rely on a fully reduced Fe(II)/Fe(II) cofactor to activate dioxygen using four electrons (creating a diferryl-like Fe(IV)/Fe(IV) intermediate), and only receive two electrons in return upon oxidizing the substrate.[4] Consequently, an external source of two electrons (e.g., NADPH) is required to reduce the resulting diferric Fe(III)/Fe(III) active site back to the diferrous form. The PhnZ reaction parallels the oxidative cleavage of a carbon–carbon bond catalyzed by the mammalian enzyme *myo*-inositol oxygenase (MIOX, EC 1.13.99.1) (Scheme 1(b)).[5] PhnZ may be an evolutionary precursor to MIOX, as they both belong to the same superfamily (pfam01966) of metal ion-dependent phosphohydrolases that contain a strictly conserved histidine-aspartate (HD) active site motif.[6] PhnZ is specific for the (R)-configured α-hydroxy group and amino group found in **1**. For example, PhnZ will not convert (R)-1-hydroxyethylphosphonic acid or the (S) enantiomer of **1**. However, PhnZ will tolerate some steric bulk at the β-carbon, as shown by conversion of (R,R)-2-amino-1-hydroxypropylphosphonic acid to Pi.[7]
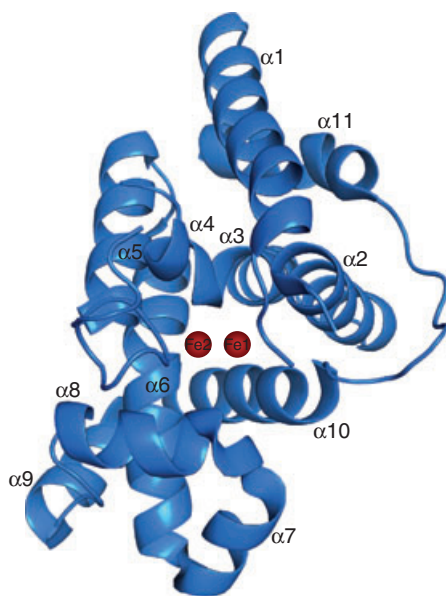
3D Structure Overview of the structure of PhnZ. Iron atoms are shown as red spheres. PDB code: 4MLN. Image produced using PyMOL.[1].
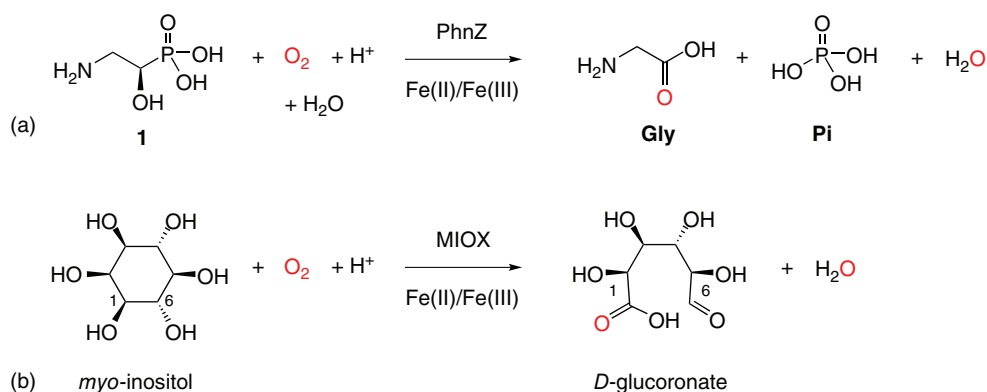
Scheme 1 (a) Reaction scheme for CP-bond cleavage by the mixed-valence di-iron oxygenase PhnZ. (b) Reaction scheme for C–C-bond cleavage by *myo*-inositol oxygenase (MIOX). The incorporation of molecular oxygen is highlighted in red. PhnZ and MIOX both belong to the 'HD' superfamily of metal ion-dependent phosphohydrolases.
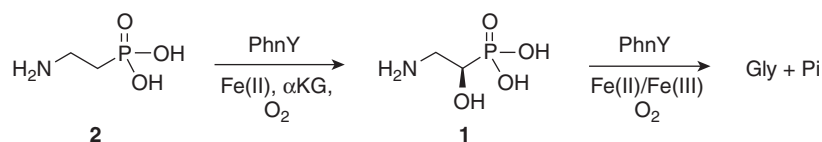
Scheme 2 Reaction scheme for the oxidative catabolism of 2-aminoethylphosphonate **2** by the tandem action of PhnY and PhnZ. This simple pathway is commonly used by marine bacteria to extract Pi from **2**.

OCCURRENCE

The gene-encoding PhnZ, where 'Phn' is short for '*phosphon*ate', was originally discovered from a marine metagenomic sample, thus its precise origin is not known.[8] However, sequence homologs of PhnZ are found in deltaproteobacteria (*Plesiocystis* sp.), cyanobacteria (*Prochlorococus marinus*), gammaproteobacteria (many species of *Pseudomonas*), CFB group bacteria (*Cyclobacterium* sp.), fungi (*Aspergillus niger*), and even a mimivirus. The latter has been proposed to be a mechanism for horizontal gene transfer of *phnZ* into different bacterial phylogenies.[8] The marine origin of PhnZ is highlighted by genome sampling data collected by the Global Ocean Survey, which found that *phnZ* is one of the most widely distributed phosphonate catabolic genes, occurring in an estimated 9.4% of marine genome equivalents.[9]

BIOLOGICAL FUNCTION

The primary role of PhnZ is to enable survival of the host bacterium in a low Pi environment. In marine and aquatic environments Pi levels can fall to low nanomolar levels.[10,11] Because Pi is a life-limiting nutrient, many microorganisms have evolved the ability to use organophosphonates (Pn)

as an alternative Pi source. Methylphosphonate and 2-aminoethylphosphonate (**2**) are two of the most abundant Pn found in marine or aquatic environments.[12,13] These often appear in strikingly high cellular concentrations as phosphonolipids, phosphonoglycans, and phosphonoglycoproteins in a variety of organisms and thus can serve as a Pi source. However, the release of Pi from Pn demands cleavage of a highly stable carbon–phosphorus bond. There are three known enzyme mechanisms for cleaving CP-bonds, namely (i) radical, found in the carbon–phosphorus lyase pathway; (ii) hydrolytic, exemplified by phosphonoacetaldehyde hydrolase (PhnX) or phosphonoacetate hydrolase (PhnA); and (iii) oxidative, represented by PhnZ.[14–17] The CP-bond of **2** can ultimately be cleaved by all three mechanisms. In the oxidative mechanism, stereospecific α-hydroxylation of **2** is first performed by PhnY, an α-ketoglutarate/non-heme iron-dependent dioxygenase, yielding the PhnZ substrate **1** (Scheme 2). Interestingly, *phnZ* is often found in seemingly redundant association with genes encoding the CP lyase pathway (*phn* operon) or the hydrolytic pathways (*phnA* or *phnX*).[8] Moreover, *phnZ* occasionally appears without *phnY* in bacterial genomes, suggesting that substrate **1** is provided by another enzyme or that in certain environmental niches, *phnY* is not necessary. The latter is certainly a possibility as **1** also occurs as a head group in phosphonolipids.[18]

AMINO ACID SEQUENCE INFORMATION

Only one PhnZ polypeptide sequence has been functionally characterized.[2,7] The host bacterium was not isolated as the genes encoding PhnZ and its partner enzyme PhnY were selected from a metagenomic DNA library using a functional screen in *Escherichia coli*.[8]

• Uncultured bacterium HF130_AEPn_1: 190 amino acids.[8]

RELATIONSHIPS

By amino acid sequence homology PhnZ belongs to the HD superfamily of metal ion-dependent phosphohydrolases (pfam01966).[6] The conserved 'HD' sequence motif is used by this family of enzymes to bind a pair of active site metal ions; in the case of PhnZ, this is His58 and Asp59 (Figure 1). An additional three His residues and an Asp residue are conserved in the HD family as metal ion-binding residues. These correspond to His34, His80, His104, and Asp161 in PhnZ. Interestingly, PhnZ belongs to a subclade of enzymes within this family, called Phn-HD (TIGR03276), as the genes encoding these enzymes are frequently associated with other phosphonate catabolic genes, such as those encoding CP lyase. Three additional residues are conserved in PhnZ homologs that are not seen in other members of the HD superfamily. This corresponds to Tyr24, Glu27, and His62 of PhnZ (Figure 1). Since the discovery of the PhnZ sequence, many related PhnZ homologs forming distinct clades within the HD superfamily have been identified in GenBank.[3]

A comparison of PhnZ with more distant relatives in the HD superfamily using structure-based alignment of amino acid sequences reveals important similarities and divergences.[7] One member of the HD superfamily is the mouse enzyme MIOX. While MIOX catalyzes a reaction that is analogous to the PhnZ reaction (Scheme 1(b)), the two enzymes share little sequence homology (10% identity, 19% similarity). Despite this lack of sequence homology, MIOX (PDB ID: 2huo) is the top structural homolog for PhnZ identified by Dali.[19] The metal ion-binding residues of PhnZ are conserved in MIOX and phosphohydrolases, but Tyr24, Glu27, and His62 of PhnZ are not observed in these enzymes (Figure 2). However, the function of His62 in substrate binding is conserved in the HD superfamily, with this role served instead by a lysine or arginine side chain in MIOX and the phosphohydrolases. PhnZ utilizes His62 to bind the α-hydroxyl of (*R*)-**1**, which is possibly ionized to an alkoxide as this group is also bound to one of the active site iron atoms (Fe2). The lysine residue Lys127 of MIOX likewise is used to engage an Fe ion-bound hydroxyl group of *myo*-inositol, while the lysine or arginine residues of the phosphohydrolases are observed to engage metal ion-bound phosphoryl oxygens of their substrates. One such

phosphohydrolase is a methanopterin biosynthetic enzyme, MptB, which has been shown to require Fe(II) for activity (Figure 2).[20] The existence of this enzyme indicates that Fe(II) has served as the basis of the evolution of two distinct chemistries in the HD superfamily: Lewis acid activation of water for hydrolytic cleavage of O—P bonds and reductive activation of dioxygen for oxidative cleavage of CP-bonds.

PROTEIN PRODUCTION AND PURIFICATION

The original metagenomic *phnZ* sequence was codon optimized for expression in *E. coli*.[2] The resulting synthetic *phnZ* sequence included a sequence encoding a C-terminal hexa-histidine tag. The *phnZ* sequence was cloned into a standard *E. coli* expression plasmid (pJ401, DNA 2.0) that utilizes a T7 promoter, a *lac* operator, and encodes kanamycin resistance. Expression of *phnZ* in *E. coli* BL21 (DE3) cells from this plasmid upon induction with isopropyl β-D-1-thiogalactopyranoside (IPTG), followed by affinity purification of the encoded enzyme on a nickel(II)-nitrilotriacetic acid (NTA) column, typically yields 8 mg L^{-1} purified enzyme per liter culture. For growing crystals of PhnZ, this step is followed by passage through a size-exclusion column.

MOLECULAR CHARACTERIZATION

PhnZ has a calculated extinction coefficient of $24\,660\,M^{-1}\,cm^{-1}$ at 280 nm based on the amino acid sequence.[2] Size-exclusion chromatography of PhnZ indicates that the enzyme is monomeric in solution.[7]

METAL CONTENT OF PHNZ

The metal ion dependence and content of PhnZ were established through activity assays and inductively coupled plasma mass spectrometry (ICP-MS) analysis of the purified enzyme.[2] When synthesized heterologously in *E. coli* in standard Luria-Bertani (LB) medium and purified by affinity chromatography, PhnZ reproducibly copurifies with 1.2 ± 0.1 mol Fe per mol enzyme.[2,3] Surprisingly, PhnZ produced this way will crystallize with two iron atoms in the active site, suggesting that this metal ion is not uniformly distributed in the active sites. Ethylenediaminetetraacetic acid (EDTA) inhibits the activity of PhnZ and can be used to remove the active site metal ions. Addition of a series of metal ions (Fe^{2+}, Fe^{3+}, Co^{2+}, Mn^{2+}, Ni^{2+}, Ca^{2+}, Cu^{2+}, Zn^{2+}, or Mg^{2+}) to apo-PhnZ revealed that only Fe(II) reconstituted full PhnZ activity and that Mg^{2+} was inhibitory.[2] The requirement for Fe(II) for activity stems from the mixed-valence Fe(II)/Fe(III) oxidation state of the di-iron active site that is used during catalysis as determined by electron paramagnetic resonance (EPR) spectroscopy.[3]
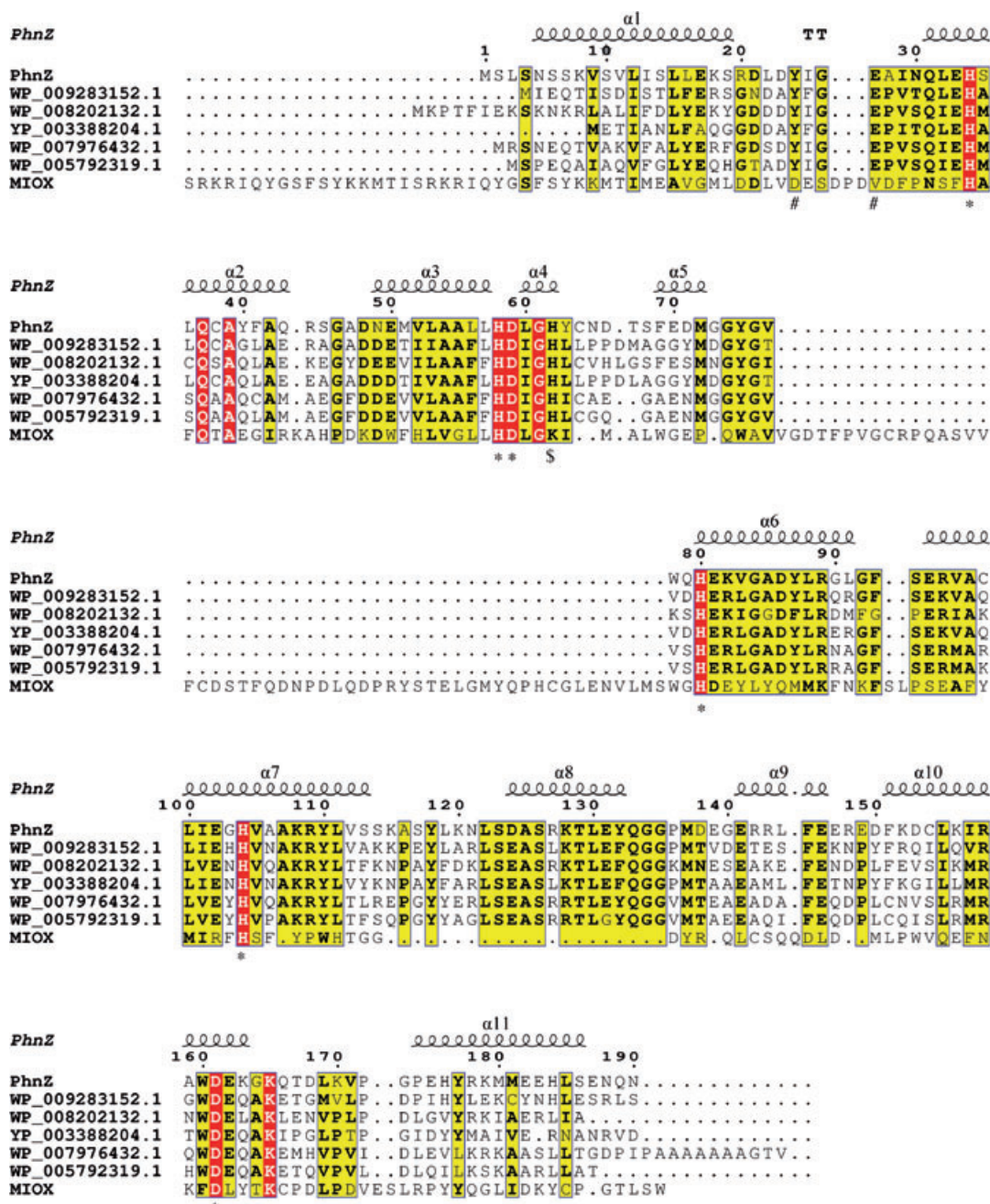
Figure 1 Amino acid sequence alignment of PhnZ with similar Phn-HD enzymes and MIOX. PhnZ (Genbank accession ACU83550) was aligned to similar enzymes from the Phn-HD subclade using Clustal Omega, then annotated with ESPript 3.0 (http://espript.ibcp.fr/ESPript/ESPript/). GenBank accession numbers are given for members of the Phn-HD subclade. Mouse *myo*-inositol-oxygenase (MIOX, Genbank accession NP_064361, PDB ID: 2huo) was structurally aligned using DaliLite and PhnZ as the reference structure. The α-helices of PhnZ are numbered and appear at the top of the alignment. Sequence numbering corresponds to PhnZ. Strictly conserved metal ion-binding residues are highlighted with asterisks (*) at the bottom of the alignment. The conserved Phn-HD subclade residues that correspond to Y24, E27, and H26 in PhnZ are highlighted with # and $ symbols at the bottom of the alignment.

Mössbauer spectroscopy was used to determine that aerobically purified PhnZ containing ^{57}Fe is initially in an inactive Fe(III)/Fe(III) state.[3] The active Fe(II)/Fe(III) form of PhnZ can be formed by adding a reducing agent (ascorbate)[3] or excess Fe(II) (0.2 mM) to a reaction solution.[7]

ACTIVITY ASSAYS

The activity of PhnZ can be monitored through the use of an enzyme-coupled assay, end-point assays, and ^{31}P NMR spectroscopy. It is important to generate the mixed-valence

```
           20        *  *            40                  60              #     80
           |                          |                   |                     |
PhnZ    LSNSSKVSVLISLLEKSRDLDYIGEAINQLEHSLQCAYFAQRSGADNEMVLAALLHDLGHYCNDTSFEDMGGYGVWQHEKVGADYLRGLGF
2huo    -------MTIMEAVGMLDDLVDESVDFPNSFHAFQTAEGIRKAHPKDWFHLVGLLHDLGKI--MALWGEP-QWAVWGHDEYLYQMMKFNKF
2pq7    -----HLREILNIVREFKDYDDP---AHDISHTFRVXENASEIASLQKAIIAALLHDIKRP--HEALTG------VDHAESGAEYASGLL-
3ccg    -----SYDKITDYLXNLGE--------KRYKHSLGVXDTAVRLADTEKARIAGLVHDCAKK---LPGEK-----SYLHGLAGRILAKKIGI
3hc1    --PDIVL-AIVDLFKT--KGPL-----TLWAHSLGVARIAKLIAEPVNVYVAGLLHDVGEVFIFFRGEFSQVV--TSHCEVGFALAKRWSL
2o08    -------GKALQLVKPHLT------HRYQHTIGVXETAIDLADQQKAELAAIFHDYAKF-RDKN---LFYGDELLHAPCGAYYVREVGI
2ogi    ---GLDRTELLSKVRHXXS--------KRFNHVLGVERAAIELADKEKAGLAALLHDYAKE--LSDD----GNNIWHGLVGIYKIQELAI
MptB    ...........................LIEHTISVTKIALKMAD.DYIIAGALLHDIMKP.............LDHLTLAVAELYKRDF


           100       120        140                 160             180
           |          |          |                   |               |
PhnZ    SERVACLIEGHVAAKRYLVSSKYLKNLSDASRKTLEYQGGPMDGERRLFEEREDFKDCLKIRAWDEKGKQTDLKVPGPEHYRKMMEEHLSE
2huo    PSEAFYMIRFHSF-YPWHTGG------------------DYRQLCSQDLD--MLPWVQEFNKFDLYTKCPDLPDVLRPYYQGLIDKYCP-
2pq7    VAEVSKAIRSHRTP-------------------------------------TSLTGKILQDADRLDAIGAV------------------
3ccg    DEDVLNAIEFHTTG---------------------------------------PNXSLLEKIIYIADYIEGREF-----------------
3hc1    NEFICDTILYHHDIEA-------------------------VPYKQA-AIVAXVAFADEYCTLRRRAAVD--------------
2o08    EEDVLQAIRFHTTG---------------------------------------PNXSLLEKIIFLADYIENRQF-----------------
2ogi    KQDILAAIAKHTVG------------------------------SAQX--STLDKIVYVADYIENRDF------------------
MptB    PIEVIKIVASHHGDH------------------------------------RPNSIEAYIVHYADEADSKINDVAVR--------------
```
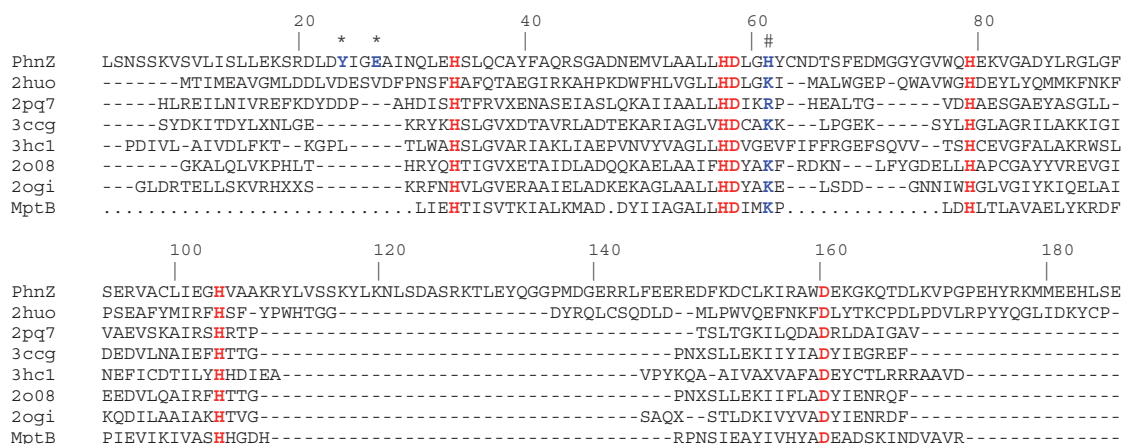
Figure 2 Structure-based sequence alignment of PhnZ with phosphohydrolases from the HD superfamily. The PhnZ sequence is aligned with the top structural homologs identified by Dali. PDB codes correspond to the following enzymes: 2huo, mouse *myo*-inositol oxygenase; 2pq7, predicted HD superfamily hydrolase from an uncultured *Thermotogales* bacterium; 3ccg, predicted HD superfamily hydrolase from *Clostridium acetobutylicum*; 3hc1, predicted HD superfamily hydrolase from *Geobacter sulfurreducens*; 2o08, predicted HD superfamily hydrolase from *Bacillus halodurans*; 2ogi, predicted HD superfamily hydrolase from *Streptococcus agalactiae*. The sequence for *M. jannaschii* phosphodiesterase MptB (Genbank accession Q58247) was aligned manually. Conserved HD superfamily metal ion-binding residues are highlighted in red. PhnZ residues Y24 and E27 are indicated with *, while H62 is indicated with #, and all are highlighted in blue. PhnZ numbering is indicated above the sequences.

Fe(II)/Fe(III) form of the cofactor to observe PhnZ activity. This is achieved simply by either adding freshly prepared ferrous iron (0.2 mM) to assay solutions[7] or by adding ascorbate,[3] which can selectively convert the inactive Fe(III)/Fe(III) form of the cofactor to the active mixed-valence form. The CP-bond cleaving activity of PhnZ can be readily monitored by detection of the Pi released during the reaction. For kinetic analysis, it is convenient to use a continuous assay for Pi.[7] This can be achieved by coupling the production of Pi with a phosphorolysis reaction catalyzed by purine nucleoside phosphorylase (PNPase) and the synthetic substrate β-D-ribosyl-1-(2-amino-6-mercapto-7-methylpurine), also known as methylthioguanosine or MESG.[21] The coupling enzyme and substrate are available as a kit (EnzChek® Phosphate Assay Kit, Molecular Probes, Introgen). Reaction of PhnZ with (*R*)-**1** generates Pi, which in turn is used by PNPase as a nucleophile to react with MESG, producing α-D-ribosyl-1-phosphate and the base 2-amino-6-mercapto-7-methylpurine. Production of the latter can be monitored continuously by absorbance at $\lambda = 360$ nm. Care must be used in selecting the pH of the reaction as the sensitivity of the coupling assay is maximal between pH 6.5 and 8. Alternatively, Pi production from a PhnZ reaction can be measured in an end-point assay using Malachite Green. ^{31}P NMR spectroscopy can also be used to quickly and unambiguously determine if PhnZ catalyzes CP-bond cleavage of a substrate. This is because α-hydroxyalkylphosphonates have chemical shifts that are well downfield of the signal for Pi (e.g., $\delta = 13$ ppm for **1** relative to H_3PO_4 in D_2O). PhnZ reactions are mixed with EDTA and dithionite before ^{31}P NMR spectroscopic

analysis to minimize the effect of paramagnetic Fe(III) on the spectrum.

SPECTROSCOPY OF PHNZ
UV/vis absorption spectroscopy

Absorbance spectroscopy is a useful method to monitor a substrate-induced conformational change that alters the ligand state of the di-iron active site of PhnZ.[7] Concentrated solutions of PhnZ (ca 0.5 mM) are pink arising from an absorbance maximum at $\lambda = 510$ nm. This absorbance stems from a charge-transfer complex formed between the phenolate oxygen of the conserved residue Tyr24 and Fe1 in its ferric form. Deletion of the phenolate oxygen (Y24F) or side chains interacting with Fe1 (D161A) results in the disappearance of the $\lambda = 510$ nm absorbance. Likewise, the addition of (*R*)-**1** induces a conformational change in a loop containing residues Asp21–Asn30 that expels Tyr24 from the active site. This disrupts the charge-transfer complex and causes the $\lambda = 510$ nm absorbance to disappear.

Mössbauer spectroscopy

Mössbauer spectroscopy has provided important information on the environment of the di-iron cofactor within the PhnZ active site.[3] The Mössbauer spectrum of aerobically purified PhnZ labeled with [57]Fe is consistent with a diferric Fe(III)/Fe(III) form of the active site. In the absence of a magnetic field at 4.2 K, the spectrum consists

of a doublet centered at $\delta = 0.5$ mm s^{-1} with a quadropole splitting constant of $\Delta E_Q = 0.79$ mm s^{-1}. This is consistent with a high-spin state ($S = 5/2$) Fe(III) ion coordinated by N and O ligands (which correspond to the Tyr, His, and Asp residues observed to coordinate the Fe ions in the crystal structure). When an external magnetic field ($B = 8.0$ T) is applied to the sample, the spectrum changes in a way that can be simulated as arising from a pair of antiferromagnetically coupled Fe(III)/Fe(III) ions. Finally, upon reducing the di-iron active site with dithionite, the Mössbauer signal (4.2 K, $B = 0$ T) shifts to $\delta = 1.3$ mm s^{-1} and the quadrupole splitting constant increases to $\Delta E_Q = 3.1$ mm s^{-1}. This is interpreted as arising from a high-spin ($S = 2$) Fe(II)/Fe(II) form of the cofactor, where each iron is octahedral and bound to N and O ligands.

EPR spectroscopy

Evidence that PhnZ utilizes a mixed-valence Fe(II)/Fe(III) cofactor for catalysis was obtained using EPR spectroscopy. Upon exposing fully reduced Fe(II)/Fe(II) PhnZ to a limiting amount of oxygen, or reducing Fe(III)/Fe(III) PhnZ with ascorbate, the Fe(II)/Fe(III) mixed-valence state of the enzyme can be stably generated.[3] The EPR spectra of such samples exhibit g values of 1.93, 1.79, and 1.68, consistent with an antiferromagnetically coupled pair of Fe(II)/Fe(III) ions. Such mixed-valence di-iron clusters are unstable in other di-iron oxygenases, such as methane monooxygenase, which rely on a fully reduced Fe(II)/Fe(II) cofactor for catalysis. Addition of substrate (*R*)-**1** to Fe(II)/Fe(III) PhnZ in the absence of dioxygen (to avoid turnover) results in a marked change to the EPR spectrum. This change can also be observed on a millisecond timescale under aerobic conditions. Such a spectral change is consistent with changes in ligand state of the Fe(II)/Fe(III) cluster. Two distinct changes that are observed in the crystal structure of PhnZ bound to (*R*)-**1**.[7] First, (*R*)-**1** is observed to bind to Fe2 in a bidentate mode using the phosphoryl and α-hydroxyl oxygen atoms. Second, the binding of (*R*)-**1** is accompanied by the expulsion of Tyr24, a ligand for Fe1, from the active site. The latter change is thought to free up a ligand site on Fe1 for binding of dioxygen. Upon addition of dioxygen to the Fe(II)/Fe(III) form of PhnZ, conversion of (*R*)-**1** to Pi is observed by ^{31}P NMR spectroscopy.[3] It is unlikely that the Fe(II)/Fe(II) form of PhnZ is catalyzing the reaction as this form is in low abundance (about 4%) in these samples and is additionally unstable toward aerobic conditions, rapidly oxidizing to the more stable Fe(II)/Fe(III) mixed oxidation state.[3]

From these experiments it is still not clear what the specific oxidation state of each Fe atom is before binding substrate. The most straightforward interpretation would have Fe2 in a ferric state to bind (*R*)-**1**, as greater Lewis acidity of this oxidation state would favor stronger substrate binding and possibly ionization of the substrate α-hydroxyl

group. Likewise, Fe1 needs to be in ferrous form to reduce and activate dioxygen. However, it is also possible that before substrate binding, the oxidation states are reversed, with Tyr24 forming a strong ligand interaction with Fe1 in ferric form and Fe2 in a substrate-free ferrous form. In this case, binding of (*R*)-**1** to Fe2 could trigger an electron transfer from Fe2 to Fe1, weakening the interaction with Tyr24 and promoting its expulsion from the active site. This model would account for the strict conservation of Tyr24 in PhnZ sequence homologs and the observation of a charge-transfer absorbance spectrum.[7] In either scenario, EPR spectroscopy provides strong evidence that the mixed-valence Fe(II)/Fe(III) state is the catalytically competent form of cofactor.[3]

X-RAY CRYSTAL STRUCTURES
Crystallization

PhnZ was independently crystallized by Bollinger and coworkers[3] and Jia and coworkers.[7] The conditions of the Jia lab, described below, led to crystals that diffracted to higher resolution and afforded more detail concerning conformational changes and substrate recognition. A selenomethionine derivative of PhnZ was purified and crystals were subsequently grown under aerobic conditions at room temperature using the hanging drop vapor diffusion method. The final crystallization condition contained ammonium sulfate, L-tartrate, and *n*-octyl-β-D-glucoside. Crystals produced by this condition were orthorhombic, belonged to the space group P2$_1$2$_1$2 with unit cell dimensions $a = 104.7$ Å, $b = 74.1$ Å, and $c = 60.7$ Å, and contained two molecules of PhnZ in the asymmetric unit. The final structure of PhnZ determined by X-ray analysis of one of these crystals was solved to 1.7 Å resolution. In parallel, PhnZ was cocrystallized with a racemic mixture of the substrate **1**, under aerobic conditions at room temperature using the sitting drop vapor diffusion method. A pre-equilibrated PhnZ substrate mixture (1:20 molar ratio) was combined in a 1:1 ratio with the well solution, which contained bis(2-hydroxyethyl)amino-tris(hydroxymethyl)methane (Bis-Tris), pH 6.5, and polyethylene glycol (PEG) 5000 monomethyl ether. Crystals produced by this condition were orthorhombic, belonged to the space group P2$_1$2$_1$2$_1$ with unit cell dimensions $a = 66.6$ Å, $b = 74.9$ Å, and $c = 75.8$ Å, and also contained two molecules of PhnZ in the asymmetric unit. The final structure of PhnZ from this crystal was solved using molecular replacement (based on the first structure) to a final resolution of 2.1 Å.

Overall structure

Two molecules of PhnZ appeared in the crystal asymmetric unit and form a dimeric interaction.[7] The PhnZ monomers are denoted molecules A and B in the following text for

clarity. Dimerization appears to be enforced by the crystal lattice as PhnZ is a monomer in solution. Each PhnZ monomer consists of a single domain made up of 11 α-helices. At the core of PhnZ, five helices, α2/α3, α5/α6, and α10, provide the residues for coordination of the two iron atoms. This α-helical core is very similar to that of MIOX, including the conservation of several metal-binding residues and their geometries. A major structural difference between MIOX and PhnZ is that the active site of MIOX is more closed to solvent than that of PhnZ. In PhnZ, access to the active site appears to be mediated by a conformational change involving the movement of two loops upon substrate binding. Further details about the di-iron active site and conformational changes are described below.

Complexes of PhnZ with the crystallization buffer additive, L-tartrate, and the substrate (R)-**1** were independently obtained. [7] In both PhnZ complexes, clear electron density is observed for two metal ions in the active site (denoted Fe1 and Fe2) along with the ligand (L-tartrate or (R)-**1**) bound to Fe2 in a bidentate mode. It is notable that only (R)-**1** is observed in the active site even though racemic **1** was used for co-crystallization. This agrees with activity assays that show that PhnZ is specific for this enantiomer.[3,7] The X-ray crystal structure of PhnZ has also been solved to 1.8 Å resolution with citrate bound to Fe2 in a bidentate mode.[3]

The di-iron active site

The two iron atoms in the PhnZ active site are coordinated by a number of amino acid side chains contributed by the nearby antiparallel helices α2/α3 and α5/α6, as well as α10. The two Fe ions are bridged by Asp59 (of the HD motif) through the carboxylate oxygens Oδ1 and Oδ2, as well as by either a water or hydroxide molecule. In both molecules of the PhnZ-tartrate structure and molecule A from the PhnZ-(R)-**1** structure, these ions are separated by similar distances of 3.76, 3.72, and 3.74 Å. However, a larger distance of 3.83 Å was observed between the two ions in molecule B of the (R)-**1**-bound structure. The active site ligands for both Fe1 and Fe2 remain consistent in both the tartrate and (R)-**1**-bound structures of PhnZ, with one exception. In both molecules of the PhnZ-tartrate structure and molecule B of the PhnZ-(R)-**1** structure, Fe1 is bound in a distorted octahedral geometry by Tyr24, His34, His58, Asp59, Asp161, and the bridging water molecule (Figure 3(a) and (c), middle and bottom panels). However, in molecule A of the PhnZ-(R)-**1** structure, Tyr24 is no longer a ligand for Fe1 and is instead replaced by a water molecule. As for Fe2, it is coordinated in an octahedral geometry by Asp59, His80, His104, and the bridging water molecule (Figure 3(b), middle and bottom panels). In the PhnZ-tartrate structure, the two remaining coordination sites are occupied by the carboxylate and α-hydroxyl oxygen of L-tartrate, whereas in the PhnZ-(R)-**1** structure, these sites are similarly occupied by a phosphoryl oxygen and the

α-hydroxyl of (R)-**1**. The conserved residue His62, which is analogous to Lys127 in MIOX, possibly mediates the ionization of the α-hydroxyl oxygens of L-tartrate and (R)-**1**.

Conformational changes upon substrate binding

Both molecules of the PhnZ-tartrate complex are nearly identical with an overall root mean square deviation (r.m.s.d.) of 0.3 Å. Similarly, molecules A and B of the PhnZ-(R)-**1** structures are almost identical with an overall r.m.s.d. of 0.8 Å. However, less similarity is seen between molecule A of the PhnZ-tartrate complex and either of the molecules from the PhnZ-(R)-**1** complex, as seen by an overall r.m.s.d. of 1.7 and 1.5 Å for molecule A and B of the PhnZ-(R)-**1** complex, respectively. The increase in r.m.s.d. is largely due to the movement of two loops that occurs upon substrate binding. With (R)-**1** bound in the active site, the first loop, composed of His62–His80, undergoes a large movement of 17 Å that is accompanied by the formation of an additional turn in the α3 helix. Ultimately this places the His62–His80 loop over the active site opposite to another loop comprising the residues Asp21–Asn30 (Figure 3, top panel, purple loop). The Asp21–Asn30 loop surrounds the active site and adopts a different conformation in each molecule of the PhnZ-(R)-**1** complex (Figure 3, top panel, magenta loop). In both molecules of the PhnZ-tartrate complex, the Asp21–Asn30 loop adopts a similar 'open' conformation in which the active site is more accessible to bulk solvent. This 'open' conformation is similar to that observed in molecule B of the PhnZ-(R)-**1** complex. The latter complex may represent a precatalytic form of the enzyme because both Fe ions are hexacoordinate and thus cannot bind molecular oxygen to carry out the oxidation of (R)-**1**.

A catalytic form of PhnZ appears to arise through a substrate-induced conformational change. A second conformation was observed in molecule A of the PhnZ-(R)-**1** complex where the Asp21–Asn30 loop adopts a 'closed' conformation in which the active site is closed off from bulk solvent (Figure 3(b), top panel). The absence of electron density that is observed for residues Ile25-Asn30 in the loop suggests that it is highly mobile when it is in the open conformation (Figure 3(c), top panel). The movement of this loop appears to be mediated by interactions between the loop residues Tyr24 and Glu27 with Fe1 and (R)-**1**, respectively. Tyr24 is the apical ligand for Fe1 in both molecules of the tartrate-bound structure and molecule B of the (R)-**1**-bound structure. In molecule A of the (R)-**1**-bound structure, Tyr24 is no longer a ligand for Fe1 and projects away from the active site. The expulsion of Tyr24 from the active site is likely caused by the entry of another residue along the loop, Glu27, into the active site. The amino group of (R)-**1** interacts electrostatically with Glu27 and is additionally solvated by two water molecules. (Figure 3(b), bottom panel). A water molecule is also observed at the apical coordination site of Fe1, previously
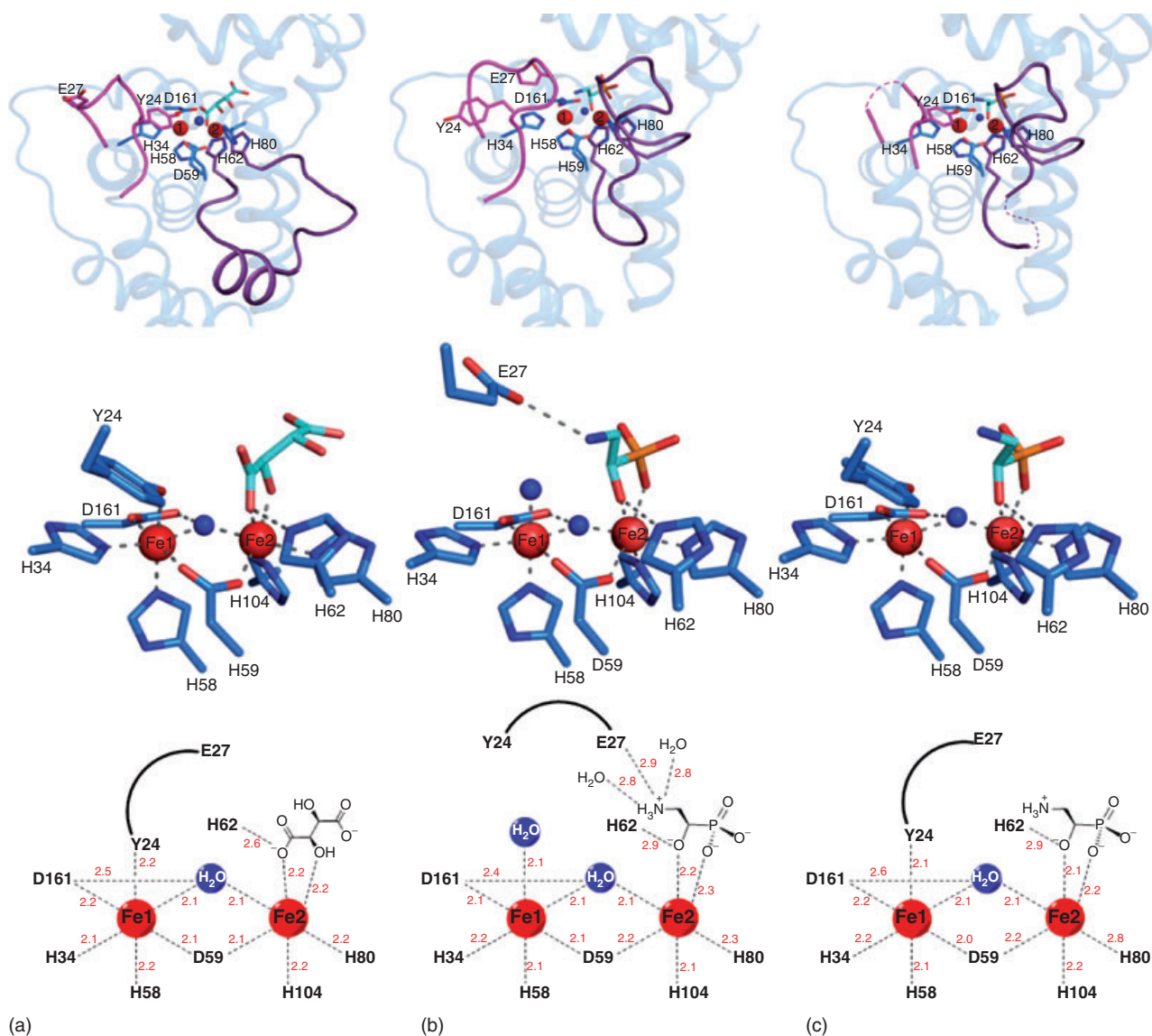
Figure 3 Active site structures and schemes of PhnZ in complex with L-tartrate and (R)-1. (a) Molecule A of the PhnZ-tartrate complex, (b) molecule A of the PhnZ-(R)-1 complex, and (c) molecule B of the PhnZ-(R)-1 complex. *Top:* overall structure of PhnZ active sites demonstrating the location of loops D21-N30 (magenta) and H62-H80 (purple), disordered residues are represented by dashes; *middle:* structural representations of each active site; *bottom:* active site schemes indicating the interatomic distances in Angstroms. Active site residues are shown as blue sticks, tartrate is shown as cyan sticks, (R)-1 is shown as cyan and orange sticks, Fe ions are shown as red spheres, and water molecules are shown as blue spheres. Top and middle panels produced using PyMol.[1]

held by the hydroxyl group of Tyr24. This water molecule is only 3.1 Å away from C1 of the substrate. Presumably this would be the binding site for molecular oxygen, placing it well within proximity to abstract the hydrogen at C1 thereby initiating oxidation of (R)-1.

FUNCTIONAL ASPECTS

Steady-state kinetic analysis of the reaction of PhnZ and several active site variants with substrate (R)-1 was performed using an enzyme-coupled assay for Pi production.

Excess Fe(II) ion (200 μM) was included in the reaction solution to maintain a di-iron FeII/FeIII active site. Classical Michaelis-Menten behavior is observed for a plot of initial rate versus concentration of (R)-1. PhnZ is a relatively slow enzyme with $k_{cat} = 11 \pm 1 \, \text{min}^{-1}$, $K_m = 0.17 \pm 0.05$ mM, and $k_{cat}/K_m = 65 \pm 20 \, \text{min}^{-1} \, \text{mM}^{-1}$ for the cleavage of (R)-1 (Table 1). Although this may seem odd for an enzyme that is serving a primary metabolic role in marine bacteria under low Pi conditions, this likely reflects the relatively slow growth rate of the host bacterium in a cold and nutrient-poor marine environment.[8] Substitution of

the two key residues Tyr24 and Glu27 produced PhnZ variants that have very different kinetic properties. PhnZ variants were designed to either improve (Y24E) or eliminate (Y24F) the ability of the side chain at position 24 to bind to Fe1. However, neither substitution had a significant effect on activity. In contrast, the PhnZ E27A variant exhibited a substantial reduction in k_{cat} (3.0 ± 0.1 min^{-1}) and increase in K_m (1.1 ± 0.1 mM) leading to a k_{cat}/K_m value (2.7 ± 0.3 min^{-1} mM^{-1}) that is only 4.1% of the wild-type enzyme value. This is interpreted as being consistent with Glu27 forming an electrostatic interaction with the 2-amino group of **1** during catalysis. Surprisingly, while PhnZ E27A retains some activity against **1**, no activity is observed in the reciprocal experiment using wild-type PhnZ and a substrate analog lacking an amino group ((R)-1-hydroxyethylphosphonic acid). So why might deleting the substrate 2-amino group of **1** be more detrimental to catalysis than deletion of the side chain of Glu27, even though both changes disrupt the electrostatic interaction between the 2-amino group of (R)-**1** and PhnZ? A clue to this paradox is provided by the X-ray crystal structure of PhnZ, which reveals two water molecules interacting with the 2-amino group of (R)-**1** along with the side chain of Glu27. Presumably, this solvation shell is absent in the case of (R)-1-hydroxyethylphosphonic acid, which may have an additional detrimental effect on substrate binding and catalysis. Interestingly, the PhnZ variants Y24F and E27A were shown by ICP-MS to purify with less Fe ion on a molar basis relative to the wild-type enzyme (Table 1). While this is consistent for a ligand role for Tyr24 with Fe1 in the absence of substrate, the result with Glu27 is unusual as this side chain does not engage a metal ion.

The Phn-HD clade of enzymes share five invariant His active site residues, unlike the rest of the HD superfamily, which only possess four that are used for metal ion binding. In the case of PhnZ, the fifth His residue corresponds to His62, which is observed to form a hydrogen bond to the α-hydroxyl group of (R)-**1**. It is likely that the hydroxyl group is ionized as it also bound to Fe2. This parallels the interaction formed between MIOX and the C6-OH of its substrate *myo*-inositol, but in this case, a lysine residue (Lys127) is used for this purpose.[26] The PhnZ H62A variant is considerably less active, with a k_{cat}/K_m value that is only 8% that of the wild-type enzyme (Table 1). This is consistent with His62 making a substantial contribution toward catalysis. It is notable that deletion of Lys127 in MIOX is also detrimental toward oxidative C–C-bond cleavage by this enzyme.[26]

The Fe ion-binding residues His34, His58, Asp59, His80, His104, and Asp161 of PhnZ are conserved in the HD superfamily. As shown in Table 1, substitution of these residues for alanine produces variants that are either unstable (D59A) or inactive toward (R)-**1** (H34A, H58A, H104A, and D161A), with the exception of H80A, which has a k_{cat}/K_m value that is 10% that of the wild-type enzyme. Interestingly, a role as a metal ion ligand does not necessarily equate with metal ion retention by PhnZ. For example, the Fe content of the H104A variant is similar to the wild-type enzyme, while the H80A and D161A variants contain less metal ion (Table 1).

THE CP-BOND CLEAVING MECHANISM OF PHNZ

The biochemical and structural analysis of PhnZ along with a detailed computational analysis of the MIOX reaction by Hirao and Morokuma[22] provides a basis to propose a hypothetical reaction mechanism for oxidative cleavage of a

Table 1 Kinetic parameters and Fe content for PhnZ and active site variants

Variant	k_{cat} (min^{-1})	K_m (mM)	k_{cat}/K_m (min^{-1} mM^{-1})	$(k_{cat}/K_m)^{var}/(k_{cat}/K_m)^{WT}$	[Fe]/[PhnZ][a]
WT	11 ± 1	0.17 ± 0.05	65 ± 20	1	1.2 ± 0.1[b]
Y24E	8 ± 1	0.22 ± 0.08	36 ± 14	0.55	—
Y24F	11 ± 1	0.26 ± 0.07	42 ± 12	0.65	0.355 ± 0.006
E27A	3.0 ± 0.1	1.1 ± 0.1	2.7 ± 0.3	0.041	0.204 ± 0.006
H62A	2 ± 1	0.4 ± 0.2	5.0 ± 3.5	0.08	—
H80A	4.0 ± 0.2	0.6 ± 0.1	6.7 ± 1.2	0.10	0.46 ± 0.01
H34A	n/d[c]	—	—	—	—
H58A	n/d	—	—	—	1.12 ± 0.04
H104A	n/d	—	—	—	—
D161A	n/d	—	—	—	0.301 ± 0.007
D59A	n/d	—	—	—	—

Parameters are reported for (R)-2-amino-1-hydroxyethylphosphonic acid **1** in the presence of 200 μM Fe(II), pH 7, 25 °C.
[a]Molar ratios of Fe and enzyme determined by ICP-MS. Values are derived from triplicate measurements.
[b]Wild-type value from reference 2.
[c]n/d = activities not determined. PhnZ variants H34A, H58A, H104A, and D161A were inactive. PhnZ D59A is unstable and precipitates during the assay.

CP-bond. At the beginning of the reaction cycle, the di-iron active site of PhnZ is proposed to be in a mixed-valence oxidation state, with Fe1 in ferric form and bound to Tyr24, while Fe2 is in ferrous form (**I** in Scheme 3). Binding of (*R*)-**1** to Fe2 may promote transfer of an electron to Fe1. The resulting ferric state of Fe2 will have greater Lewis acidity that will favor binding of the phosphoryl and α-hydroxyl oxygens of (*R*)-**1** in a bidentate manner. The binding of (*R*)-**1** to Fe2 may promote ionization of the α-hydroxyl, with His62 acting as a base (intermediate **II**). The ferrous form of Fe1 will weaken the interaction with Tyr24, which along with the specific interaction of Glu27 with the 2-amino group of (*R*)-**1**, will promote the expulsion of Tyr24 from the active site. Such an induced fit mechanism of binding (*R*)-**1** is proposed to create a vacant ligand site at Fe1 for binding and reducing dioxygen (**II–III**). The resulting Fe(III) superoxide is proposed to abstract the α-hydrogen of (*R*)-**1**. Calculations by Hirao on MIOX indicate that the resulting carbon-centered radical does not persist in this step, but instead the single electron delocalizes into Fe2 (**III–IV**). In the case of PhnZ, this would lead to formation of an acyl-phosphonate. This electrophilic intermediate is proposed to be attacked by the hydroperoxide bound to Fe1 with general base assistance provided by the di-iron bridging hydroxide (**IV–V**). The resulting Criegee-like intermediate **V** may undergo a rearrangement analogous to

a Baeyer–Villiger reaction, thus cleaving the CP-bond of **1** to form the acyl phosphate ester of glycine. However, the analogous rearrangement in the MIOX reaction has been calculated by Hirao to be of higher energy than homolytic cleavage of the peroxide bond without alkyl group migration. This step is calculated to be rate determining for MIOX.[22] In the context of PhnZ, this would lead to generation of a ferryl oxygen at Fe1 and a geminal diolate intermediate (**V–VI**). The ferryl oxygen is proposed to abstract the hydroxyl hydrogen of **VI**, with the resulting hydroxy radical promoting the cleavage of the β-CP-bond and elimination of a phosphonyl radical (**VII–VIII**). The latter is proposed to reduce Fe2 back to the ferrous state, with the resulting meta-phosphate attacked by water to form Pi. The β-elimination of a phosphonyl radical by a hydroxy radical (**VII–VIII**) is certainly feasible and this same reaction has been applied to acylphosphonates to synthesize carbon–carbon bonds.[23,24]

The proposed mechanism accounts for several experimental observations. First, this mechanism explains the strict conservation of Tyr24, Glu27, and His62 in PhnZ homologs. It explains the charge-transfer complex that is observed between Tyr24 and Fe1, as well as how this complex is disrupted by the binding of (*R*)-**1**. The substantial changes in the EPR spectrum for PhnZ that is observed upon binding (*R*)-**1** are also consistent with this model.[3]
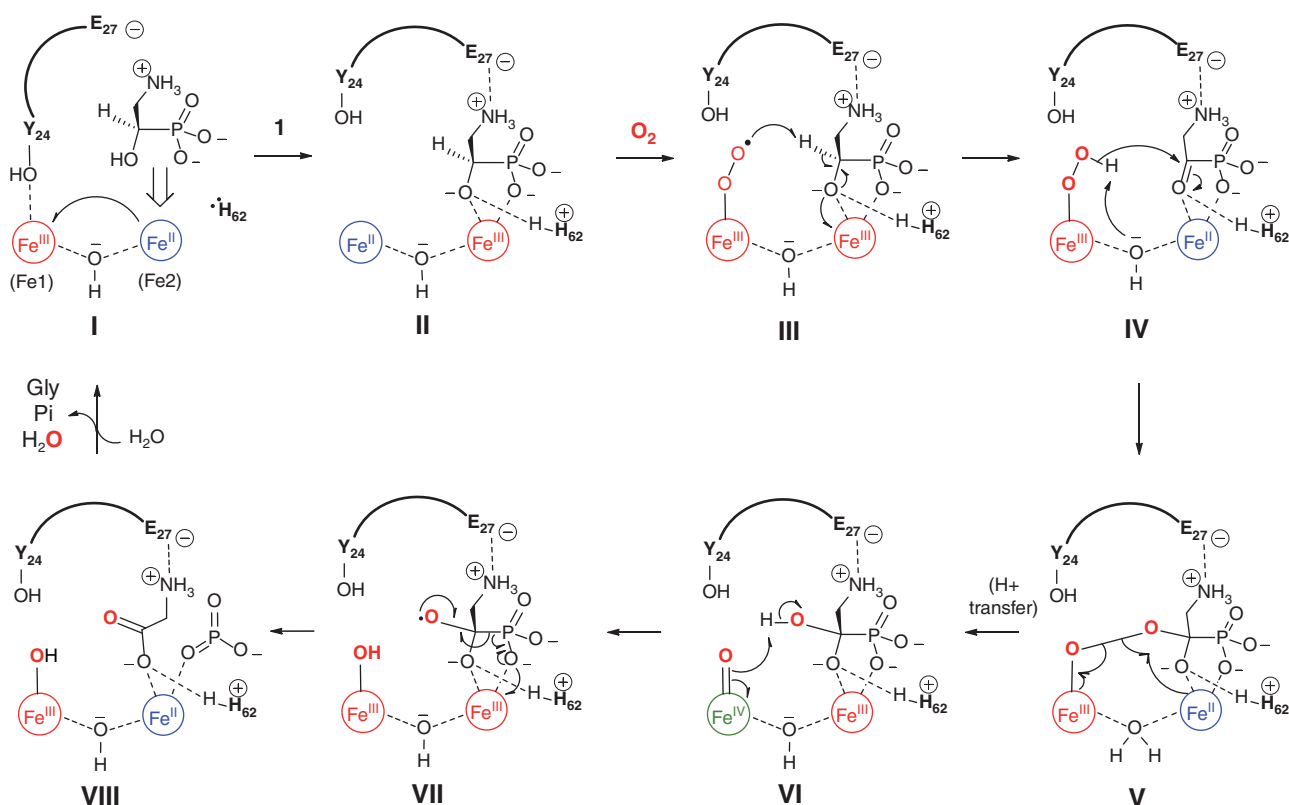
Scheme 3 Mechanism for the oxidative cleavage of the CP-bond by PhnZ.

This induced fit model of substrate binding is substantiated by the conformational changes observed in the X-ray crystal structure of PhnZ bound to (*R*)-**1**. Moreover, the observations that deletion of the Tyr24 hydroxyl has a negligible effect on the reaction rate, while deletion of the side chains of Glu27 or His62 have significant effects, are consistent with Tyr24 fulfilling a place-holder role for dioxygen, while Glu27 and His62 are actively engaged with the substrate during catalysis. Finally, the mechanism accounts for the surprisingly small primary deuterium kinetic isotope effect that is observed with (*R*)-**1** labeled with deuterium at the α carbon ($k_H/k_D = 1.36 \pm 0.06$; Séguin, Pallitsch, Vogt, Hammerschmidt, Zechel, unpublished). The C—H-bond cleavage step (**III–IV**) may only be partly rate limiting if peroxide-bond cleavage to form the ferryl oxygen (**V–VI**) is kinetically significant, as implied by the calculations by Hirao.[22] Interestingly, a negligible primary deuterium KIE is also observed in the MIOX reaction,[25] suggesting PhnZ and MIOX share a conserved rate-limiting step.

RELATED ARTICLES

Iron: Heme Proteins, Mono- & Dioxygenases; Iron: Models of Proteins with Dinuclear Active Sites; Iron Proteins with Dinuclear Active Sites; Iron Proteins with Mononuclear Active Sites; Mössbauer Spectroscopy; Phosphorus: Organophosphorus Chemistry; Modeling Metalloenzymes with Density Functional and Mixed Quantum Mechanical/Molecular Mechanical (QM/MM) Calculations: Progress and Challenges; Dioxygenase; Enzyme; Methane Monooxygenase Hydroxylase; Iron: Non-Heme Proteins with Diiron-Carboxylate Active Sites; Dinuclear Iron Cluster-Containing Oxygenase CmlA

REFERENCES

1   DeLano WL, The PyMol Molecular Graphics System, DeLano Scientific, San Carlos, CA (2002).

2   FR McSorley, PB Wyatt, A Martinez, EF DeLong, B Hove-Jensen and DL Zechel, *J Am Chem Soc*, **134**, 8364–8367 (2012).

3   B Wörsdörfer, M Lingaraju, NH Yennawar, AK Boal, C Krebs, JM Bollinger and ME Pandelia, *Proc Natl Acad Sci U S A*, **110**, 18874–18879 (2013).

4   CE Tinberg and SJ Lippard, *Acc Chem Res*, **44**, 280–288 (2011).

5   JM Bollinger, Y Diao, ML Matthews, G Xing and C Krebs, *Dalton Trans*, 905–914 (2009).

6   L Aravind and EV Koonin, *Trends Biochem Sci*, **23**, 469–472 (1998).

7   LM van Staalduinen, FR McSorley, K Schiessl, J Seguin, PB Wyatt, F Hammerschmidt, DL Zechel and Z Jia, *Proc Natl Acad Sci U S A*, **111**, 5171–5176 (2014).

8   A Martinez, GW Tyson and EF DeLong, *Environ Microbiol*, **12**, 222–238 (2010).

9   J Villarreal-Chiu and J Quinn, *Front Microbiol*, **3**, 1–13 (2012).

10 BAS Van Mooy, HF Fredricks, BE Pedler, ST Dyhrman, DM Karl, M Koblížek, MW Lomas, TJ Mincer, LR Moore, T Moutin, MS Rappé and EA Webb, *Nature*, **458**, 69–72 (2009).

11 ST Dyhrman, PD Chappell, ST Haley, JW Moffett, ED Orchard, JB Waterbury and EA Webb, *Nature*, **439**, 68–71 (2006).

12 WW Metcalf, BM Griffin, RM Cicchillo, J Gao, SC Janga, HA Cooke, BT Circello, BS Evans, W Martens-Habbena, DA Stahl and WA van der Donk, *Science*, **337**, 1104–1107 (2012).

13 WW Metcalf and WA van der Donk, *Annu Rev Biochem*, **78**, 65–94 (2009).

14 JW McGrath, JP Chin and JP Quinn, *Nat Rev Microbiol*, **11**, 412–419 (2013).

15 SC Peck and WA van der Donk, *Curr Opin Chem Biol*, **17**, 1–9 (2013).

16 SS Kamat and FM Raushel, *Curr Opin Chem Biol*, **17**, 589–596 (2013).

17 B Hove-Jensen, FR McSorley and DL Zechel, *PLoS One*, **7**, e46416 (2012).

18 ED Korn, DG Dearborn, HM Fales and EA Sokoloski, *J Biol Chem*, **248**, 2257–2259 (1973).

19 L Holm and P Rosenström, *Nucleic Acids Res*, **38**, W545–W549 (2010).

20 Z Mashhadi, H Xu and RH White, *Biochemistry*, **48**, 9384–9392 (2009).

21 MR Webb, *Proc Natl Acad Sci U S A*, **89**, 4884–4887 (1992).

22 H Hirao and K Morokuma, *J Am Chem Soc*, **131**, 17206–17214 (2009).

23 S Kim, CH Cho and CJ Lim, *J Am Chem Soc*, **125**, 9574–9575 (2003).

24 D Leca, L Fensterbank, E Lacôte and M Malacria, *Chem Soc Rev*, **34**, 858–865 (2005).

25 G Xing, Y Diao, LM Hoffart, EW Barr, KS Prabhu, RJ Arner, CC Reddy, C Krebs and JM Bollinger, *Proc Natl Acad Sci U S A*, **103**, 6130–6135 (2006).

26 PM Brown, TT Caradoc-Davies, JMJ Dickson, GJS Cooper, KM Loomes, EN Baker, *Proc Natl Acad Sci USA*, **103**, 15032–15037 (2006).